

# Chemical Science

Accepted Manuscript

This article can be cited before page numbers have been issued, to do this please use: Z. G. Walters, D. C. Witkowski, K. N. Houk and N. K. Garg, *Chem. Sci.*, 2025, DOI: 10.1039/D5SC03943F.



This is an Accepted Manuscript, which has been through the Royal Society of Chemistry peer review process and has been accepted for publication.

Accepted Manuscripts are published online shortly after acceptance, before technical editing, formatting and proof reading. Using this free service, authors can make their results available to the community, in citable form, before we publish the edited article. We will replace this Accepted Manuscript with the edited and formatted Advance Article as soon as it is available.

You can find more information about Accepted Manuscripts in the [Information for Authors](#).

Please note that technical editing may introduce minor changes to the text and/or graphics, which may alter content. The journal's standard [Terms & Conditions](#) and the [Ethical guidelines](#) still apply. In no event shall the Royal Society of Chemistry be held responsible for any errors or omissions in this Accepted Manuscript or any consequences arising from the use of any information it contains.

# Mechanisms of Kobayashi Eliminations for the Generation of Highly-Strained Arynes, Cyclic Cumulenes, and Anti-Bredt Olefins†

View Article Online  
DOI: 10.1039/D5SC03943F

Received 00th January 20xx,  
Accepted 00th January 20xx

DOI: 10.1039/x0xx00000x

Zach G. Walters,<sup>‡a</sup> Dominick C. Witkowski,<sup>‡a</sup> K. N. Houk,<sup>a</sup> and Neil K. Garg<sup>\*a</sup>

First disclosed in 1983, the Kobayashi method for generating transient strained intermediates from 1,2-silyltriflate precursors, has become an indispensable tool in organic synthesis. More than 1,300 Kobayashi precursors to strained intermediates have been reported to date, leading to the use of these precursors in more than 17,000 strained intermediate trapping reactions. Surprisingly, the mechanism of the Kobayashi elimination to form strained intermediates has been studied only for the formation of benzyne. We report computational studies that determine the timing of Si–C and C–O cleavage, as well as the thermodynamics of strained intermediate formation. The calculated pathway for generating anti-Bredt olefins from Kobayashi precursors differs compared to the mechanism for strained intermediate generation of other species, with a particular dependence on the Si–C–C–O dihedral angle. These studies establish the mechanisms of Kobayashi eliminations and enable the rational design of new strained intermediate precursors for future use in synthesis.

## Introduction

Arynes and related strained intermediates have become common building blocks in organic synthesis.<sup>1,2,3,4</sup> Despite being historically avoided and having short lifetimes, such transient species have shown value in many areas, such as natural product synthesis,<sup>5,6</sup> heterocycle synthesis,<sup>7,8</sup> medicinal chemistry,<sup>9</sup> ligand synthesis,<sup>10</sup> organometallic and materials chemistry,<sup>11,12</sup> agrochemistry,<sup>13</sup> DNA-encoded library synthesis,<sup>14</sup> and more.<sup>15</sup> Thousands of studies of such intermediates have been reported, with the field continuing to inspire new developments in synthesis.

A key technological advance that has fueled the widespread use of arynes and related strained intermediates in modern synthesis is the discovery of 1,2-silyltriflate precursors to strained intermediates.<sup>16</sup> This strategy was first reported by Kobayashi and coworkers in 1983 and is highlighted in Fig. 1A.<sup>16</sup> Reaction of silyltriflate **1** with furan (**2**) in the presence of tetramethylammonium fluoride (Me<sub>4</sub>NF) delivers cycloadduct **4**, presumably through the intermediacy of benzyne (**3**).

This methodology was first applied to the preparation of benzyne, but it has been extended to the preparation of many other strained intermediates, such as other arynes,<sup>17,18,19</sup> non-aromatic cyclic alkynes,<sup>20,21,22</sup> cumulated alkenes (such as cyclic allenes and cyclic 1,2,3-trienes),<sup>23,24,25,26,27,28,29</sup> and anti-Bredt olefins<sup>30</sup> (see **5–12**, Fig. 1B). More than 1,300 distinct Kobayashi precursors to alkenes and alkynes are known,<sup>31</sup> including heterocyclic Kobayashi precursors (e.g., **13–16**),<sup>32,33,34,35</sup> which have collectively been deployed in more than 17,000 reactions reported in the literature.<sup>31</sup> Factors that have rendered the Kobayashi methodology so practical include: a) mild conditions for strained intermediate generation; b) functional group compatibility; c) safe use;<sup>36</sup> d) enablement of different modes of reactivity (including pericyclic reactions, nucleophilic additions, annulations, cascade and tandem reactions, multi-component reactions, metal-catalysed reactions,<sup>37,38</sup> and  $\sigma$ -bond insertions<sup>39</sup>); and e) the aforementioned versatility in accessing distinct strained intermediate classes. Of note,

transformations of strained intermediates generated from Kobayashi precursors commonly form two bonds, and are increasingly used to access structurally- and stereochemically-complex products.<sup>2,4</sup>

What are the mechanisms of Kobayashi eliminations for formation of strained arynes, cycloalkynes, cumulenes and alkenes? Many theoretical studies of arynes and related intermediates exist, but these largely focus on structure and reactivity of the strained intermediates. For example, studies of ground state geometries,<sup>40,41,42</sup> strain,<sup>43,44,45,46</sup> energy of dehydrogenation,<sup>47</sup> reaction kinetics,<sup>30,39,48,49</sup> regioselective trapings,<sup>25,28,34,35,50,51</sup> and further computational studies of trapping reactions are known.<sup>52,53,54</sup> In contrast, how and why the Kobayashi elimination takes place has been reported in just two prior computational studies of the formation of benzyne.<sup>55,56</sup> The aforementioned Yu *et al.* study was performed at the B3LYP/6-31G(d) level of theory and Biju *et al.* with M06-2X-D3/6-31G(d,p); both predict fluoride attack to give a pentavalent silicate anion as the rate determining step, with subsequent Si–C cleavage having a small barrier and C–O cleavage negligible, leaving considerable uncertainty about the E2 or E1cB mechanism of the elimination. Furthermore, the mechanisms by which other classes of strained intermediates, such as cyclic alkyne **5**, cyclic allene **7**, cyclic 1,2,3-triene **9** and anti-Bredt olefin **11** are formed from Kobayashi precursors have not been studied computationally.

We report computational studies of the mechanisms of Kobayashi eliminations to form strained intermediates (**17a** or **17b** → **18a** or **18b** using fluoride (**19**), Fig. 1C). Density functional theory (DFT) calculations of the thermodynamics of formation of several distinct classes of strained intermediates are reported, along with mechanisms of generation of **3**, **5**, **9** and **11**.<sup>57</sup> Although the fluoride-promoted elimination of the 1,2-silyltriflate motif ensures favourable thermodynamics in all cases, different elimination mechanisms are operative depending on the substrate. These studies not only serve to determine reaction mechanisms for Kobayashi eliminations, but provide guidance for the rational design of new strained intermediate precursors for use in synthesis.

<sup>a</sup> Department of Chemistry and Biochemistry, University of California at Los Angeles, Los Angeles, California 90095, United States. E-mail: neilgarg@g.ucla.edu

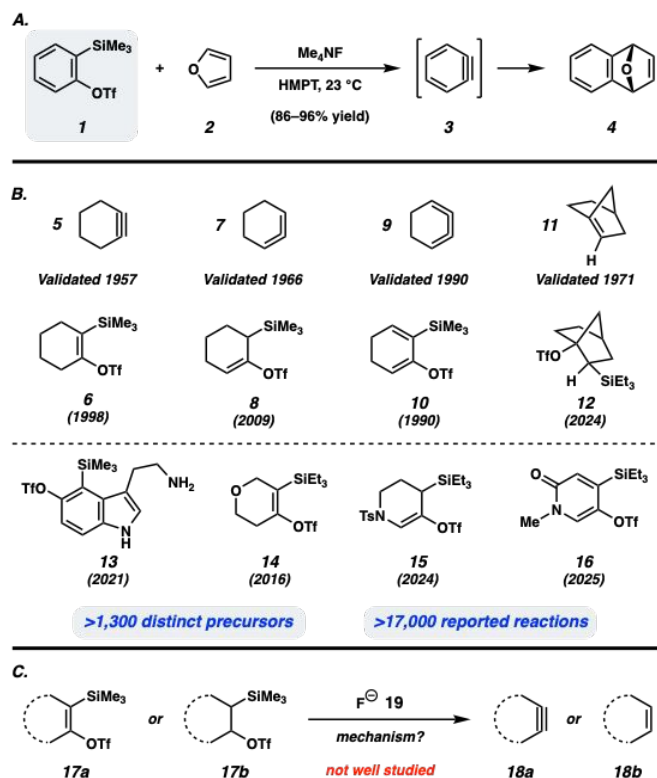
†Electronic supplementary information (ESI) available. See DOI: 10.1039/x0xx00000x

‡ These authors contributed equally to this work.



## ARTICLE

## Chemical Science



## Results and Discussion

## Thermodynamics of Kobayashi eliminations to form strained intermediates

The transient intermediates depicted in Fig. 1A and 1B, each validated many decades ago,<sup>24,58,59,60</sup> are well known to possess significant strain energies, ranging from ~30 to >50 kcal mol<sup>-1</sup>.<sup>30,43,45,46</sup> Nonetheless, Kobayashi eliminations can be used to access these high-energy species at ambient temperatures. We have computed the thermodynamics of formation of these strained intermediates *via* Kobayashi's fluoride-promoted elimination from different precursors.

As shown in Fig. 2, we examined reactions where a Kobayashi precursor, generally shown as **17a** or **17b**,<sup>61</sup> is reacted with fluoride (**19**) to form alkynes **18a** or alkenes **18b**, respectively. The process is accompanied by the loss of Me<sub>3</sub>SiF (**20**) and the triflate anion (**21**). This process was studied using DFT calculations, at the ωB97X-D/def2-QZVPP//ωB97X-D/6-31+G(d,p) level of theory, using SMD models of solvents used in experiments. This high level of theory was recently used to study aryne generation, albeit *via* a different base-mediated elimination mechanism.<sup>62,63</sup> We are only aware of computations of the thermodynamics for the generation of benzyne from a Kobayashi precursor,<sup>55,56</sup> whereas the corresponding computations for the generation of other strained cyclic intermediates (e.g., nonaromatic alkynes, cumulated alkenes, and anti-Bredt olefins) have not been reported.

Results from the computational evaluation of thermodynamic favourability are summarized in Fig. 2. Beginning with the Kobayashi

elimination of **1** to give benzyne (**3**), the reaction is calculated to be exergonic by 8.8 kcal mol<sup>-1</sup> (entry 1).<sup>64</sup> The generation of cyclohexyne (**5**) from **6** is even more thermodynamically favourable, (ΔG = -22.6 kcal mol<sup>-1</sup>, entry 2) which is reasonable given the reduced strain present in **5** relative to **3**.<sup>22,46</sup> The generation of 1,2-cyclohexadiene (**7**) from precursor **8** is also computed to be energetically favourable (entry 3).<sup>57</sup> The more negative ΔG of -31.7 kcal mol<sup>-1</sup> again is in line with reduced strain of **7**, relative to **3** or **5**.<sup>45</sup> We also considered the generation of 1,2,3-cyclohexatriene (**9**) and anti-Bredt olefin **11** (entries 4 and 5, respectively). Whereas the thermodynamics for the generation of **9** are akin to that of benzyne (**3**) (ΔG = -3.3 kcal mol<sup>-1</sup>, entry 4), the formation of anti-Bredt olefin **11** from silyltriflate **22** is energetically downhill by 21.2 kcal mol<sup>-1</sup> (entry 5).

Several lessons are as follows: a) computations on the thermodynamics for Kobayashi generation of various strained intermediates generally correlate with experimental findings; b) for similar types of strained intermediates, the relative ΔG values are generally consistent with relative strain energies; c) the formation of Me<sub>3</sub>SiF (**20**) and the loss of a suitable leaving group (*i.e.*, triflate anion **21**; pK<sub>a</sub> TfOH ca. -15) are essential for the success of these reactions; and d) although different leaving groups can be used in Kobayashi eliminations,<sup>2</sup> the use of a silicon species and fluoride to trigger strained intermediate formation is essential, presumably due to the pronounced strength of the forming Si-F bond (Bond dissociation energy (BDE) ≅ 135 kcal mol<sup>-1</sup>).<sup>65</sup> Lastly, for practitioners designing new Kobayashi precursors to strained intermediates, the straightforward computations of the type shown in Fig. 2 are an excellent method to assess thermodynamic feasibility, prior to embarking on experiments.



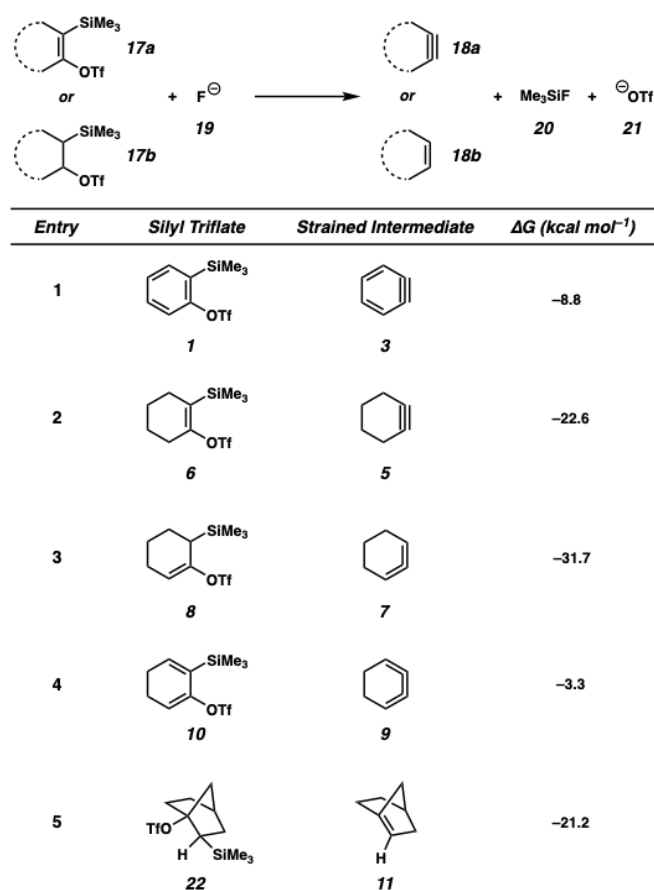


**Fig. 2**  $\Delta G$  values for the fluoride-mediated generation of strained intermediates from their trimethylsilyltriflate precursors. All energies are reported in kcal mol<sup>-1</sup>. Calculations were performed at the  $\omega$ B97X-D/def2-QZVPP/SMD(solvent)// $\omega$ B97X-D/6-31+G(d,p)/SMD(solvent) level. Solvent = MeCN for entries 1–3, DMSO for entry 4, and toluene for entry 5 to mimic experimental conditions.

### Kobayashi elimination to form benzyne (3).

As noted earlier, computational studies of aryne trapping processes are well-known; however, studies pertaining to how arynes (and other strained intermediates) are actually generated from Kobayashi precursors are sparse, with seminal contributions by Li & Yan in 2017<sup>55</sup> and by Jindal & Biju in 2021.<sup>56</sup> Thus, we first computed the energy profile for the reaction of silyltriflate **1** with fluoride (**19**) to generate benzyne (**3**) (Fig. 3). Although this has been computed previously using B3LYP/6-31G(d),<sup>55</sup> we sought to examine the transformation using a higher level

of theory ( $\omega$ B97X-D/def2-QZVPP/SMD(MeCN)// $\omega$ B97X-D/6-31+G(d,p)/SMD(MeCN)), consistent with the computational methods used earlier in the present study.<sup>62</sup> Indeed, the more advanced functional used here predicts an overall free energy change of -9 kcal mol<sup>-1</sup> versus the earlier value of -31 kcal mol<sup>-1</sup> obtained using B3LYP.<sup>55</sup>

As shown in Fig. 3, addition of fluoride (**19**) to silyltriflate **1**, gives pre-complex **23**. From **23**, formation of silicate **24** proceeds via **TS-1** ( $\Delta G^\ddagger = 9.4$  kcal mol<sup>-1</sup>). Silicate **24** then undergoes dissociation via **TS-2** ( $\Delta G^\ddagger = 7.5$  kcal mol<sup>-1</sup>) to furnish anion **25**. The loss of Me<sub>3</sub>SiF<sup>66</sup> (**20**) provides a driving force for the reaction (10.4 kcal mol<sup>-1</sup> downhill), given the notable strength of the Si–F bond<sup>65</sup> as discussed earlier. Benzyne (**3**) is then formed via elimination of triflate anion **21** from **25** via **TS-3**, with a barrier ( $\Delta G^\ddagger$ ) of 5.7 kcal mol<sup>-1</sup>. The overall reaction of silyltriflate **1** and fluoride anion (**19**) to give benzyne (**3**), Me<sub>3</sub>SiF (**20**), and triflate anion **21** is thermodynamically favourable by 8.8 kcal mol<sup>-1</sup> as previously discussed.

We also considered an alternative pathway from **25** that has occasionally been observed experimentally for silyltriflates in specialized cases, which is the thia-Fries rearrangement to give phenoxide **26** (Fig. 3).<sup>67,68,69,70</sup> The mechanism of the thia-Fries rearrangement was expected to also proceed via aryl anion **25**, lending some support for the intermediacy of **25** since it is common to both pathways (i.e., aryne formation and thia-Fries rearrangement).<sup>71</sup> We examined this rearrangement mechanism and identified **TS-4** as a plausible transition state. However, the barrier ( $\Delta G^\ddagger$ ) for this process is 15.2 kcal mol<sup>-1</sup> and formation of benzyne (**3**) is favoured by 9.5 kcal mol<sup>-1</sup> ( $\Delta\Delta G^\ddagger$ ). This explains why thia-Fries rearrangement is typically not observed in reactions of silyltriflate **1** under standard Kobayashi elimination conditions, but may be observed in other systems.<sup>72</sup>

Several additional considerations should be noted. First, a concerted, E2-like transition state that would allow for the direct conversion of silicate **24** to benzyne (**3**), via postulated **TS-5**, was not found (Fig. 3). In addition, the elimination of **25** to form **3** has a barrier of only 5 kcal mol<sup>-1</sup>. As proposed in Kobayashi's seminal report,<sup>16</sup> the barrier to elimination is likely less than the barrier for the bimolecular reaction that would be required for protonation of **25**, especially given the aprotic reaction conditions typically used in experiments. With the hope of finding experimental support for the intermediacy of **25**, we have performed aryne generation experiments in the presence of excess *t*-BuOH and indeed observe the formation of some aryltriflate.<sup>73</sup> Overall, we conclude that the Kobayashi elimination to form benzyne (**3**) involves aryl anion **25** as a key intermediate and proceeds via an E1cB-type mechanism, whereas the direct elimination from silicate **24** to give benzyne (**3**) is disfavoured.



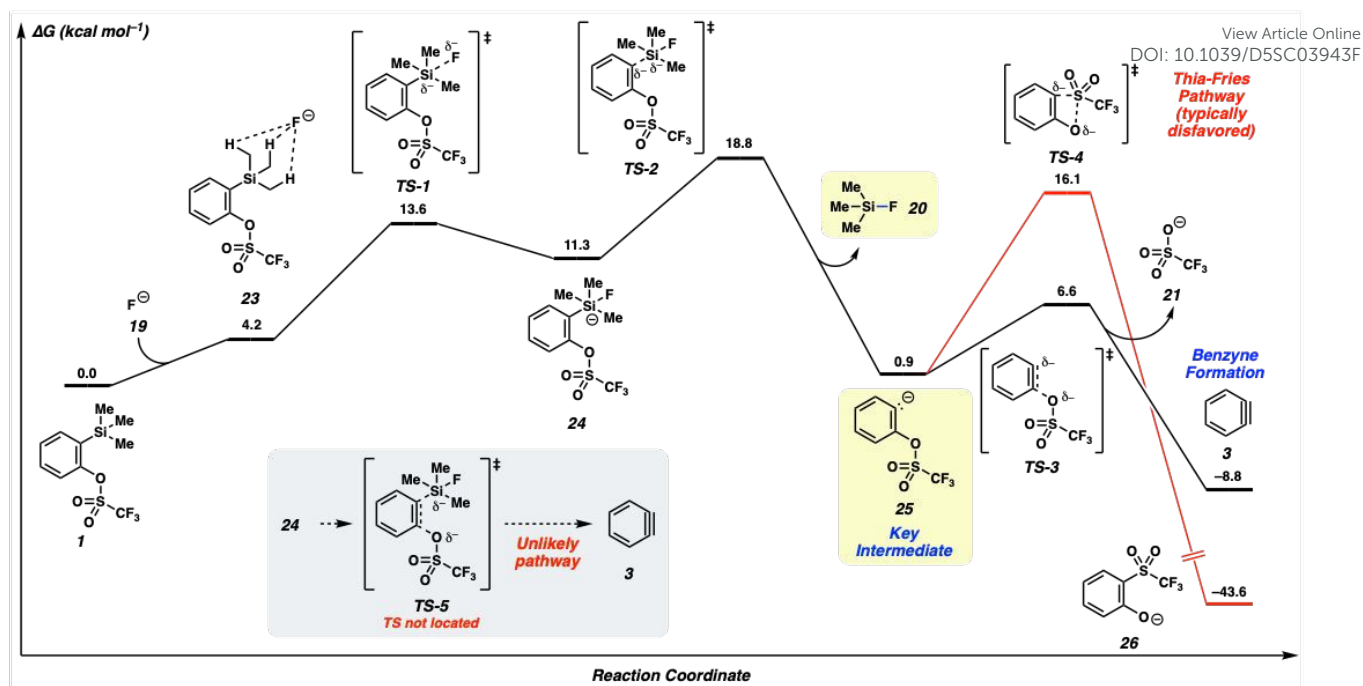


**Fig. 3** Calculated energy profile for the fluoride-mediated elimination of silyltriflate **1** to generate benzyne (**3**) (ωB97X-D/def2-QZVPP/SMD(MeCN)//ωB97X-D/6-31+G(d,p)/SMD(MeCN)). All energies are reported in kcal mol<sup>-1</sup>

### Mechanisms of Kobayashi eliminations to form cyclohexyne (**5**) and 1,2,3-cyclohexatriene (**9**)

Despite possessing differing functional groups (*i.e.*, alkyne vs. cumulene), cyclohexyne (**5**) and 1,2,3-cyclohexatriene (**9**) are conceptually similar to benzyne (**1**), in that each possesses: a) a functional group that ordinarily prefers a linear geometry, but is bent due to ring constraints; and b) a highly reactive  $\pi$  bond that is essentially orthogonal to the other alkene or alkenes present in the strained intermediate. Kobayashi precursors to these intermediates and their derivatives have been reported, along with their use in many cycloaddition reactions.<sup>20,22,24,25</sup>

As the mechanisms for the Kobayashi eliminations to give **5** or **9** from **6**<sup>20</sup> or **10**<sup>24</sup>, respectively, have not been reported previously, we studied both computationally (Fig. 4). The energy profiles were determined to be very similar to what we calculated for benzyne (**3**; see Fig. 3) and the full reaction coordinate diagrams are available in the ESI (sections F and G, respectively). Most notably, for both pathways, computations support a

mechanism involving silicate formation (not shown), generation of a discrete carbanion (**27** or **28**) with formation of Me<sub>3</sub>SiF (**20**), followed by loss of the triflate anion (**21**) to give the strained intermediate (*via* transition state **TS-6** or **TS-7**).<sup>74</sup> We note the following findings: a) The formation of **20** and **21** are important driving forces for these processes, leading to the overall reactions being downhill by 22.6 and 3.3 kcal mol<sup>-1</sup> respectively, as noted earlier (see Fig. 2); b) In the case of cyclohexyne (**5**), elimination of vinyl anion intermediate **27** is a barrierless pathway, whereas the corresponding elimination of vinyl anion intermediate **28** proceeds with an activation barrier ( $\Delta G^\ddagger$ ) of 6.9 kcal mol<sup>-1</sup>; c) This difference is rationalized by comparing the relative strain energies of the two intermediates (~40 kcal mol<sup>-1</sup> vs ~50 kcal mol<sup>-1</sup> for **5** vs **3**, respectively), and is consistent with the relative exothermicities ( $\Delta G$ ) of the eliminations; and d) Finally, we calculated similar reaction energy profiles and mechanisms for the Kobayashi eliminations to give two other 1,2,3 cyclic trienes, including an azacyclic 1,2,3-triene<sup>35</sup> (see the ESI, section I).





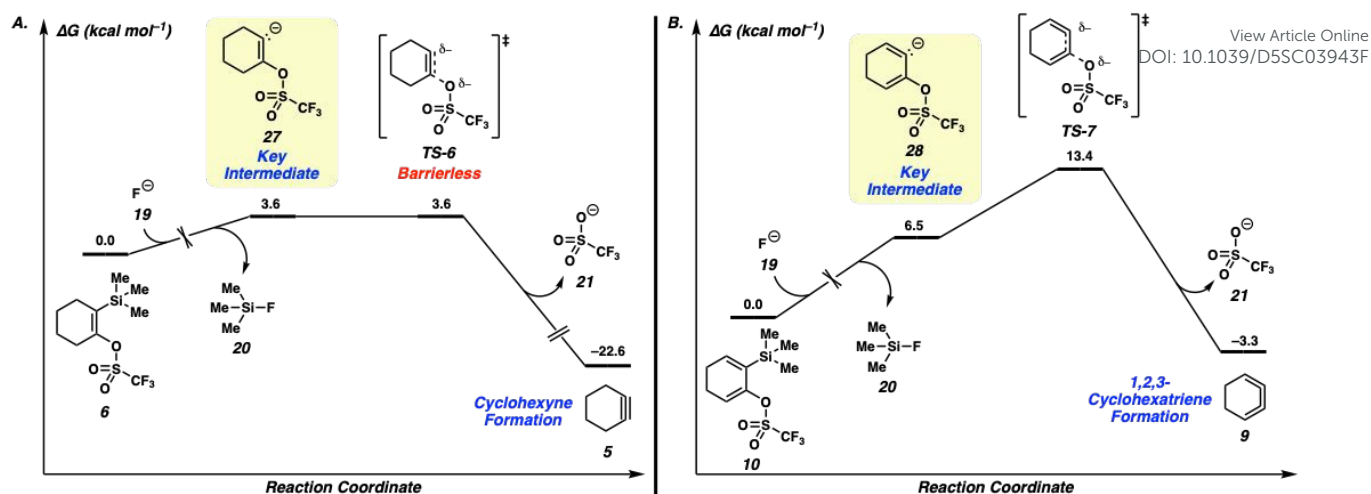


**Fig. 4** (A) Abbreviated energy profile for the generation of cyclohexyne (5) ( $\omega$ B97X-D/def2-QZVPP/SMD(MeCN)//( $\omega$ B97X-D/6-31+G(d,p)/SMD(MeCN)). All energies are reported in kcal mol<sup>-1</sup>. (B) Abbreviated energy profile for the generation of 1,2,3-cyclohexatriene (9) ( $\omega$ B97X-D/def2-QZVPP/SMD(MeCN)//( $\omega$ B97X-D/6-31+G(d,p)/SMD(MeCN)). All energies are reported in kcal mol<sup>-1</sup>.

### Kobayashi eliminations to form anti-Bredt olefins.

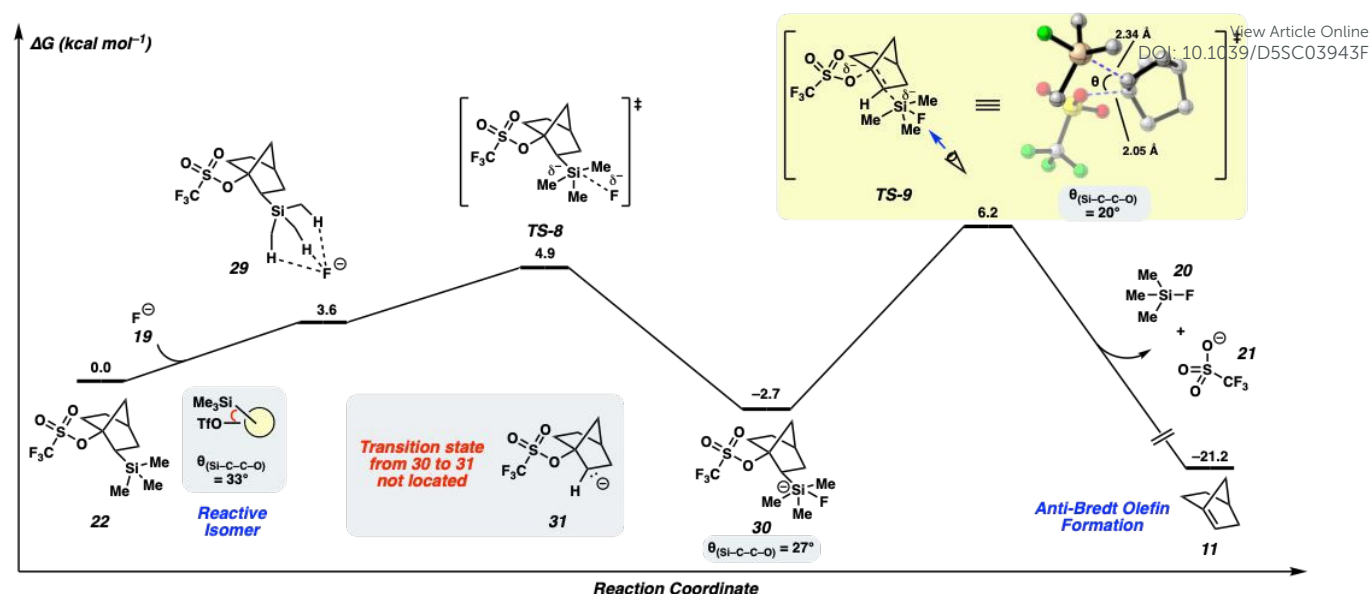
Another intriguing class of Kobayashi precursors are those that allow for the generation of anti-Bredt olefins. The Kobayashi approach to anti-Bredt olefins was only recently disclosed<sup>29</sup> as a general method to overcome Bredt's rule and access alkenes that possess severe geometric distortion. A unique aspect of Kobayashi precursors to anti-Bredt olefins is that the substrates typically bear both the silicon and leaving group substituents on saturated carbons. This leads to variations in the relationship of the Si-C and C-O bonds, as well as lower stability of the presumed carbanion that would be generated if Si-C bond cleavage occurred, prior to alkene formation, as seen in the aforementioned cases. We have examined the Kobayashi elimination to generate anti-Bredt olefin **11**, including stereochemical ramifications, computationally.

Fig. 5 shows the calculated free energy profile and mechanism for the reaction of silyltriflate **22** to give [2.2.1] anti-Bredt olefin **11**. The feasibility of this overall conversion is supported by experiments.<sup>29</sup> Beginning with **22**, the Si-C-C-O dihedral angle is 33°. Addition of fluoride anion (**19**), via precomplex **29**, leads to transition state **TS-8**, with

a very small overall barrier of 4.9 kcal mol<sup>-1</sup>. Formation of silicate **30** is exergonic by 2.7 kcal mol<sup>-1</sup>.

From **30**, we examined two pathways for generating anti-Bredt olefin **11**. One pathway, the E1cB mechanism, involves formation of carbanion **31**, which would be akin to the pathways found for the other strained intermediates discussed earlier (see benzyne (**3**), cyclohexyne (**5**), 1,2,3-cyclohexatriene (**9**); Figs. 3 and 4). However, a transition state to arrive at carbanion **31** from **30** could not be located, which is reasonable considering that carbanion **31** would be unstabilized and highly disfavoured.<sup>75,76</sup> Regarding the alternative pathway, silicate **30** is calculated to undergo facile E2-type elimination through **TS-9**, with an activation barrier ( $\Delta G^\ddagger$ ) of 8.9 kcal mol<sup>-1</sup>, to give anti-Bredt olefin **11**. Of note, as the reaction proceeds, there is a progressive contraction of the Si-C-C-O dihedral angle ( $\theta$ ), beginning at 33° in **22**, decreasing to 27° in silicate **30**, and finally adopting an angle of 20° in **TS-9**. This suggests a strong stereo-electronic requirement for Kobayashi elimination on strictly aliphatic systems. As noted earlier, the overall process is 21.2 kcal mol<sup>-1</sup> downhill, driven by the energetically favourable release of Me<sub>3</sub>SiF (**20**) and the triflate anion (**21**).





**Fig. 5** Mechanism and energy profile for the fluoride-mediated generation of anti-Bredt olefin **11** from silyltriflate **22** (ωB97X-D/def2-QZVPP/SMD(toluene)//ωB97X-D/6-31+G(d,p)/SMD(toluene)). All energies are reported in kcal mol<sup>-1</sup>.

We also performed computations of the epimeric Kobayashi precursor, **epi-22**, with select results shown in Fig. 6. In this unreactive substrate, the Si–C–O dihedral angle is 72°. Silicate **epi-30** can be generated analogously to **30** (see ESI, section K for further details); however, this was found to be an unproductive intermediate. More specifically, transition states leading to concerted 1,2-elimination or formation of a discrete carbanion could not be located. Direct elimination of the silicate, which is predicted to occur for epimer **30** (see Fig. 5), is presumably not feasible for **epi-30** due to poor orbital overlap between the breaking C–Si σ orbital and C–O σ\* orbital of the breaking bond, as the Si–C–O dihedral angle in silicate **epi-30** is 70°. Overall, these calculations are consistent with **epi-22** not undergoing fluoride-mediated Kobayashi elimination experimentally<sup>29</sup> and further underscore the importance of the Si–C–O dihedral angle in allowing for generation of the strained intermediate.

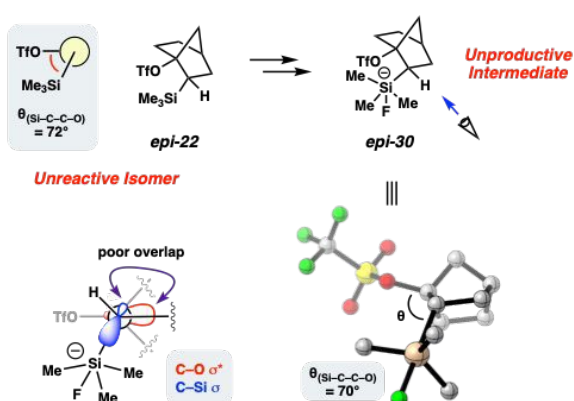


**Fig. 6** Study of unreactive substrate (**epi-22**) under fluoride-mediated conditions ((U)ωB97X-D/def2-QZVPP/SMD(toluene)//(U)ωB97X-D/6-31+G(d,p)/SMD(toluene)).

### Study of impact of dihedral angle on Kobayashi eliminations of aliphatic systems.

In order to further understand the importance of the Si–C–O dihedral angle for successful Kobayashi elimination to generate strained cyclic alkenes, such as anti-Bredt olefins, we performed computations involving the simplest silyltriflate, **32**, as a model (Fig. 7A).<sup>77</sup> Kobayashi elimination of this model system would give ethylene (**34**). By systematically constraining the Si–C–O dihedral angles (θ) from 180° (*anti*-periplanar) to 0° (*syn*-periplanar), we could determine the impact of dihedral angle on the transition state barrier for elimination. Thus, optimized structures of silyltriflates **32** and their corresponding silicate anions **33** were calculated for structures with θ constrained to 180°, 0°, and angles at 15° intervals within those boundaries.<sup>78</sup> Additionally, concerted elimination transition states **TS-10** were located for each constrained silicate **33** to give ethylene (**34**).

Fig. 7A shows a plot of the ΔG of the transition state for elimination across the dihedral angles examined. Barriers are lowest for *anti*- or *syn*-eliminations, where θ is constrained to roughly 180° (**TS-10a**, ΔG ≅ 11 kcal mol<sup>-1</sup>) or 0° (**TS-10c**, ΔG ≅ 13 kcal mol<sup>-1</sup>), as these orientations lead to optimal overlap between the C–Si σ orbital and the C–O σ\* orbital. *Anti*-elimination pathways (*i.e.*, **TS-10a**) are most favourable, as is generally known for E2 eliminations.<sup>79</sup> The activation barrier for Kobayashi elimination increases dramatically as θ approaches 90° (**TS-10b**, ΔG ≅ 22 kcal mol<sup>-1</sup>), reflective of poor orbital overlap in the transition state for elimination and the high strain of the eventual product with p orbitals oriented in an approximately perpendicular fashion.

**TS-10a**, **TS-10b**, and **TS-10c** are shown in Fig. 7B. The transition state geometries show very similar bond lengths in the favourable transition states **TS-10a** (θ = 180°) and **TS-10c** (θ = 0°). The breaking C–Si bond is 2.11 Å in both cases, whereas the breaking C–O bond is 1.69 Å or 1.74 Å, respectively. In contrast, the C–Si and C–O bonds in the disfavoured



transition state **TS-10b** are elongated to 2.16 Å and 1.93 Å, respectively, indicative of a later transition state.

Finally, computations on plausible Kobayashi precursors of constrained aliphatic substrates are a valuable predecessor to substrate synthesis, since they can reveal difficulties that might arise in achieving

the elimination.<sup>80</sup> The geometries seen in such Kobayashi precursors tend to be similar to that seen in the intermediate silicates formed after fluoride addition and, therefore, reasonably approximate the expected Si–C–C–O dihedral. Dihedral angles between 180–120° and 35–0° are appropriate for successful Kobayashi eliminations

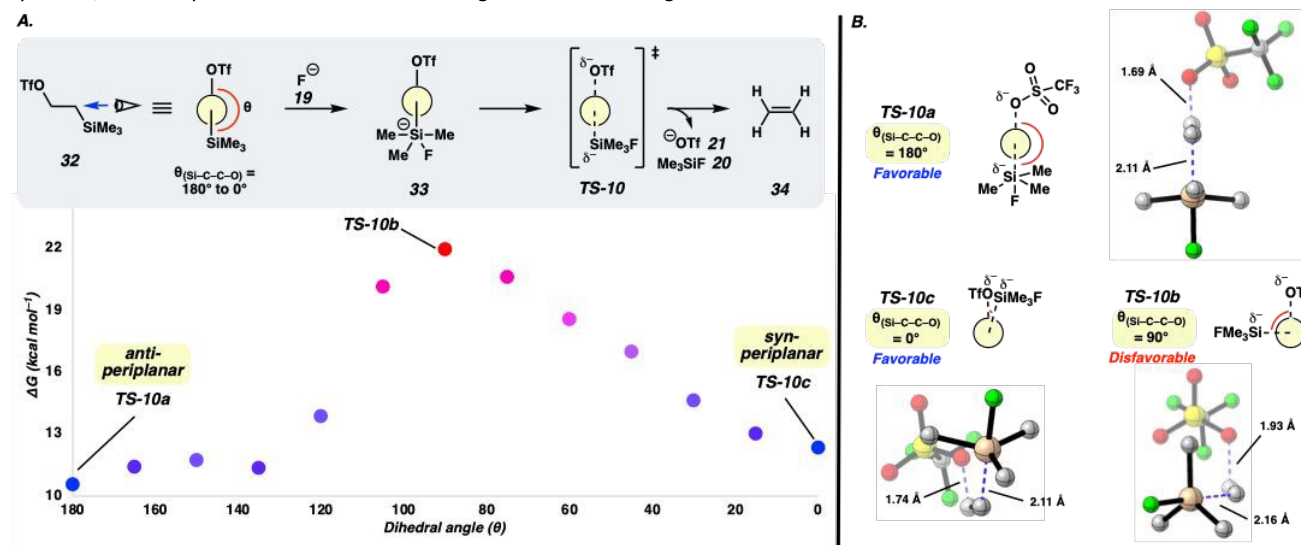


**Fig. 7.** (A) Computational study of fluoride-mediated generation of ethylene (**34**) from silyltriflate **32** with varying Si–C–C–O dihedral angles  $\theta$  (ωB97X-D/def2-QZVPP/SMD(MeCN)//ωB97X-D/6-31+G(d,p)/SMD(MeCN)). (B) Key transition states **TS-10a-c** and geometric parameters. All energies are reported in kcal mol<sup>-1</sup>.

## Conclusions

Kobayashi precursors to strained intermediates have become valuable building blocks in organic synthesis, resulting in >17,000 chemical reactions, with applications across numerous fields. Kobayashi precursors to arynes, cyclic alkynes, cyclic 1,2,3-trienes, cyclic allenes, and strained alkenes, such as anti-Bredt olefins, have been developed. Although the formation of benzyne had been studied previously, we investigated the mechanism in detail, as well as mechanisms for other classes of strained intermediates: strained alkenes, alkynes, and 1,2,3-trienes.

We find that: a) Kobayashi eliminations, despite leading to highly strained intermediates, are thermodynamically favourable as a result of formation of the strong Si–F bond, as well as the loss of the excellent triflate leaving group; b) all mechanisms proceed *via* initial formation of a silicate anion; and c) the mechanism of elimination varies, either proceeding through desilylative carbanion formation, followed by elimination (for arynes, cyclic alkynes, and cyclic 1,2,3-trienes), or direct elimination of the silicate anion (for anti-Bredt olefins) in cases where the intermediate carbanion is highly unstable, so that triflate anion loss occurs with breaking of the Si–C bond. In the latter case, stereoelectronic requirements dictate the barrier of elimination.

Our studies help to inform the future design of Kobayashi precursors. We recommend that, prior to experiment, one calculate the thermodynamic feasibility of the conversion of the proposed Kobayashi precursor to the corresponding strained intermediate. Such calculations are relatively straightforward, not requiring transition state analysis, but

provide important insight that can be used to encourage or discourage specific experiments. This process may be particularly useful in considering substituted versions of the strained intermediates we study here, as well as new strained intermediates that have not yet been generated using the Kobayashi approach. With regard to specific mechanisms, aryne, cyclic alkyne, and cyclic 1,2,3-triene generation pathways are thought to proceed via intermediate aryl or vinyl anions that eliminate a synperiplanar leaving group. Thus, in designing substrates, one can choose where to position the silicon and the leaving group, as well as the specific silicon and leaving group substituents. Generally speaking, one need not worry extensively about other stereoelectronic effects in these aryl or alkenyl systems (i.e., compared to stereoelectronic effects in anti-Bredt olefins), although the presence of adjacent substituents could plausibly impact the stability of the intermediate aryl or vinyl anion, leading to changes in mechanism or the rate of leaving group ejection. Lastly, in the case of aliphatic Kobayashi precursors to strained alkenes, such as anti-Bredt olefins, stereoelectronic considerations become important, as such reactions are thought to not proceed via an intermediate carbanion.<sup>81</sup> It is advised to target Si–C–C–Leaving group dihedral angles between 180–120° (for trans elimination) and 35–0° (for cis elimination) in the substrate to optimize chances of successful Kobayashi elimination.

Our studies provide fundamental insight regarding the thermodynamics and mechanisms of Kobayashi eliminations, which enable the rational design of new strained intermediate precursors for future uses in synthesis.





## Data availability

Full details on the computational methods are accessible in the ESI.†

## Author contributions

Z. G. W. and D. C. W. designed, performed, and analysed computational studies. K. N. H. advised on computational findings. N. K. G. directed the computational investigation and prepared the manuscript with contributions from all authors; all authors contributed to discussions.

## Conflicts of interest

There are no conflicts to declare.

## Acknowledgements

The authors are grateful to the NIH-NIGMS (R35 GM139593 for N.K.G.), the Trueblood Family (for N.K.G.), the Foote Family (for Z.G.W.), the UCLA Graduate Division Dissertation Year Fellowship (for D.C.W.), the Stone Family (for D.C.W.), and the National Science Foundation (CHE-2153972 to K.N.H.). Calculations were performed on the Hoffman2 cluster and the UCLA Institute of Digital Research and Education (IDRE) at UCLA and the Extreme Science and Engineering Discovery Environment (XSEDE), which is supported by the National Science Foundation (OCI-1053575). These studies were supported by shared instrumentation grants from the NSF (CHE-1048804) and the NIH NCRR (S10RR025631).

## Notes and references

- 1 H. H. Wenk, M. Winkler and W. Sander, One century of aryne chemistry, *Angew. Chem., Int. Ed.*, 2003, **42**, 502–528.
- 2 J. Shi, L. Li and Y. Li, *o*-Silylaryl triflates: A journey of Kobayashi aryne precursors, *Chem. Rev.* 2021, **121**, 3892–4044.
- 3 S. M. Anthony, L. G. Wonilowicz, M. S. McVeigh and N. K. Garg, Leveraging fleeting strained intermediates to access complex scaffolds, *JACS Au*, 2021, **1**, 897–912.
- 4 L. McDermott, Z. G. Walters, A. M. Clark and N. K. Garg, Geometric distortion as an enabling tool for organic synthesis, *Nat. Synth.*, 2025, **4**, 421–431.
- 5 P. M. Tadross and B. M. Stoltz, A comprehensive history of arynes in natural product total synthesis, *Chem. Rev.*, 2012, **112**, 3550–3577.
- 6 C. M. Gampe and E. M. Carreira, Arynes and cyclohexyne in natural product synthesis, *Angew. Chem., Int. Ed.*, 2012, **51**, 3766–3778.
- 7 A. V. Dubrovskiy, N. A. Markina and R. C. Larock, Use of benzyne for the synthesis of heterocycles, *Org. Biomol. Chem.*, 2013, **11**, 191–218.
- 8 A. E. Goetz, T. K. Shah and N. K. Garg, Pyridynes and indolynes as building blocks for functionalized heterocycles and natural products,

*Chem. Commun.*, 2015, **51**, 34–45.

- 9 J. W. Coe, P. R. Brooks, M. C. Wirtz, C. G. Bashore, K. E. Bianco, M. G. Vetelino, E. P. Arnold, L. A. Lebel, C. B. Fox, F. D. Tingley, D. W. Schulz, T. I. Davis, S. B. Sands, R. S. Mansbach, H. Rollemma and B. T. O'Neill, 3,5-Bicyclic aryl piperidines: A novel class of  $\alpha 4\beta 2$  neuronal nicotinic receptor partial agonists for smoking cessation, *Bioorg. Med. Chem. Lett.*, 2005, **15**, 4889–4897.
- 10 C. C. Mauger and G. A. Mignani, An efficient and safe procedure for the large-scale Pd-catalyzed hydrazonation of aromatic chlorides using Buchwald technology, *Org. Process. Res. Dev.* 2004, **8**, 1065–1071.
- 11 J. V. Chari, K. A. Spence, R. B. Susick and N. K. Garg, A platform for on-the-complex annulation reactions with transient aryne intermediates, *Nat. Commun.*, 2021, **12**, 3706–3715.
- 12 Z.-Y. Wang, Y.-Z. Xu, Z. Cui, L. Zhang, J.-Y. Lu, Y.-Q. Zheng and R. Zhu, Chain-growth synthesis of extensively cross-conjugated polyenes, *Nat. Synth.*, 2025, DOI: 10.1038/s44160-025-00760-4.
- 13 F. Schleth, T. Vettiger, M. Rommel and H. Tobler, Process for the preparation of pyrazole carboxylic acid amides. Intl. Pat., WO 2011131544 A1, 2011.
- 14 M. V. Westphal, L. Hudson, J. W. Mason, J. A. Pradeilles, F. J. Zécri, K. Briner and S. L. Schreiber, Water-compatible cycloadditions of oligonucleotide-conjugated strained allenes for DNA-encoded library synthesis, *J. Am. Chem. Soc.*, 2020, **142**, 7776–7782.
- 15 D. Svatunek, M. Wilkovitsch, L. Hartmann, K. N. Houk and H. Mikula, Uncovering the key role of distortion in bioorthogonal tetrazine tools that defy the reactivity/stability trade-off, *J. Am. Chem. Soc.*, 2022, **144**, 8171–8177.
- 16 Y. Himeshima, T. Sonoda and H. Kobayashi, Fluoride-induced 1,2-elimination of *o*-trimethylsilylphenyl triflate to benzyne under mild conditions, *Chem. Lett.*, 1983, **12**, 1211–1214.
- 17 A. E. Goetz and N. K. Garg, Enabling the use of heterocyclic arynes in chemical synthesis, *J. Org. Chem.*, 2014, **79**, 846–851.
- 18 Y. Nakamura, S. Yoshida and T. Hosoya, Recent advances in synthetic hetaryne chemistry, *Heterocycles*, 2019, **98**, 1623–1677.
- 19 For the recent use of a Kobayashi precursor to generate a paracyclophene, see: X. Zhang, Y. Zhou, Z.-X. Yu, C.-H. Tung, Z. Xu, Strained Dehydro-[2,2]-paracyclophane Enabled Planar Chirality Construction and [2,2]Paracyclophane Functionalization, *Angew. Chem., Int. Ed.*, 2025, **64**, e202420667.
- 20 N. Atanes, S. Escudero, D. Pérez, E. Guitián and L. Castedo, Generation of cyclohexyne and its Diels-Alder reaction with  $\alpha$ -pyrones, *Tetrahedron Lett.*, 1998, **39**, 3039–3040.
- 21 S. F. Tlais and R. L. Danheiser, *N*-Tosyl-3-azacyclohexyne. Synthesis and chemistry of a strained cyclic ynamide, *J. Am. Chem. Soc.* 2014, **136**, 15489–15492.
- 22 J. M. Medina, T. C. McMahon, G. Jiménez-Oseá, K. N. Houk and N. K. Garg, Cycloadditions of cyclohexynes and cyclopentyne, *J. Am. Chem. Soc.*, 2014, **136**, 14706–14709.
- 23 I. Quintana, D. Peña, D. Pérez and E. Guitián, Generation and reactivity of 1,2-cyclohexadiene under mild reaction conditions, *Eur. J. Org. Chem.*, 2009, **2009**, 5519–5524.
- 24 W. C. Shakespeare and R. P. Johnson, 1,2,3-Cyclohexatriene and cyclohexen-3-yne: Two new highly strained  $C_6H_6$  isomers, *J. Am. Chem. Soc.*, 1990, **112**, 8578–8579.
- 25 A. V. Kellegan, A. S. Bulger, D. C. Witkowski and N. K. Garg, Strain-promoted reactions of 1,2,3-cyclohexatriene and its derivatives,



*Nature*, 2023, **618**, 748–754.

26 V. A. Lofstrand and F. G. West, Efficient trapping of 1,2-cyclohexadienes with 1,3-dipoles, *Chem. Eur. J.*, 2016, **22**, 10763–10767.

27 Y. A. Almelhadi and F. G. West, A mild method for the generation and interception of 1,2-cycloheptadienes with 1,3-dipoles, *Org. Lett.*, 2020, **22**, 6091–6095.

28 J. S Barber, M. M. Yamano, M. Ramirez, E. R. Darzi, R. R. Knapp, F. Liu, K. N. Houk and N. K. Garg, Diels–Alder cycloadditions of strained azacyclic allenes, *Nat. Chem.*, 2018, **10**, 953–960.

29 C. L. Jankovic, K. C. McIntosh, V. A. Lofstrand and F. G. West, Stereoselective intramolecular [2+2] trapping of 1,2-cyclohexadienes: A route to rigid, angularly fused tricyclic scaffolds, *Chem. Eur. J.*, 2023, **29**, e202301668.

30 L. McDermott, Z. G. Walters, S. A. French, A. M. Clark, J. Ding, A. V. Kelleghan, K. N. Houk and N. K. Garg, A solution to the anti-Bredt olefin synthesis problem, *Science*, 2024, **386**, eadq3519.

31 On the basis of a SciFinder structure search; see the ESI for details; Scifinder-n; Chemical Abstracts Service: Columbus, OH; <https://scifinder-n.cas.org> (accessed May 7, 2025).

32 S. M. Anthony, V. Tona, Y. Zou, L. A. Morrill, J. M. Billingsley, M. Lim, Y. Tang, K. N. Houk and N. K. Garg, Total synthesis of (–)-strictosidine and interception of aryne natural product derivatives “strictosidine” and “strictosamidine”, *J. Am. Chem. Soc.*, 2021, **143**, 7471–7479.

33 T. K. Shah, J. M. Medina and N. K. Garg, Expanding the strained alkyne toolbox: Generation and utility of oxygen-containing strained alkynes, *J. Am. Chem. Soc.*, 2016, **138**, 4948–4954.

34 A. V. Kelleghan, A. Tena Meza and N. K. Garg, Generation and reactivity of unsymmetrical strained heterocyclic allenes, *Nat. Synth.*, 2024, **3**, 329–336.

35 D. C. Witkowski, D. W. Turner, A. S. Bulger, K. N. Houk and N. K. Garg, Synthesis and reactivity of nitrogen-containing strained cyclic 1,2,3-trienes, *Nat. Synth.*, 2025, DOI: 10.1038/s44160-025-00793-9.

36 A. V. Kelleghan, C. A. Busacca, M. Sarvestani, I. Volchkov, J. M. Medina and N. K. Garg, Safety assessment of benzyne generation from a silyl triflate precursor, *Org. Lett.*, 2020, **22**, 1665–1669.

37 R. A. Dhokale and S. B. Mhaske, Transition-metal-catalyzed reactions involving arynes, *Synthesis*, 2018, **50**, 1–16.

38 K. A. Spence, A. Tena Meza and N. K. Garg, Merging Metals and strained intermediates, *Chem Catal.*, 2022, **2**, 1870–1879.

39 A. Tena Meza, C. A. Rivera, H. Shao, A. V. Kelleghan, K. N. Houk and N. K. Garg,  $\sigma$ -Bond insertion reactions of two strained diradicaloids, *Nature*, 2025, **640**, 683–690.

40 J. M. Medina, J. L. Mackey, N. K. Garg and K. N. Houk, The role of aryne distortions, steric effects, and charges in regioselectivities of aryne reactions, *J. Am. Chem. Soc.*, 2014, **136**, 15798–15805.

41 P. H.-Y. Cheong, R. S. Paton, S. M. Bronner, G.-Y. J. Im, N. K. Garg and K. N. Houk, Indolyne and aryne distortions and nucleophilic regioselectivities, *J. Am. Chem. Soc.*, 2010, **132**, 1267–1269.

42 G.-Y. J. Im, S. M. Bronner, A. E. Goetz, R. S. Paton, P. H.-Y. Cheong, K. N. Houk and N. K. Garg, Indolyne experimental and computational studies: Synthetic applications and origins of selectivities of nucleophilic additions, *J. Am. Chem. Soc.*, 2010, **132**, 17933–17944.

43 J. F. Liebman and A. Greenberg, A survey of strained organic molecules, *Chem. Rev.*, 1976, **76**, 311–365.

44 I. Novak, Molecular modeling of anti-Bredt compounds, *J. Chem. Inf. Model.*, 2005, **45**, 334–338.

45 K. J. Daoust, S. M. Hernandez, K. M. Konrad, I. D. Mackie, J. Winstanley and R. P. Johnson, Strain estimates for small-ring cyclic

allenes and butatrienes, *J. Org. Chem.*, 2006, **71**, 5708–5714.

46 R. P. Johnson and K. J. Daoust, Interconversions of cyclobutene, cyclopentene, cyclohexene, and their corresponding cycloalkylenecarbenes, *J. Am. Chem. Soc.*, 1995, **117**, 362–367.

47 A. E. Goetz, S. M. Bronner, J. D. Cisneros, J. M. Melamed, R. S. Paton, K. N. Houk and N. K. Garg, An efficient computational model to predict the synthetic utility of heterocyclic arynes, *Angew. Chem., Int. Ed.*, 2012, **51**, 2758–2762.

48 M. M. Yamano, A. V. Kelleghan, Q. Shao, M. Giroud, B. J. Simmons, B. Li, S. Chen, K. N. Houk and N. K. Garg, Intercepting fleeting cyclic allenes with asymmetric nickel catalysis, *Nature*, 2020, **586**, 242–247.

49 Q. Xu and T. R. Hoyer, A distinct mode of strain-driven cyclic allene reactivity: Group migration to the central allene carbon atom, *J. Am. Chem. Soc.*, 2023, **145**, 9867–9875.

50 A. E. Goetz and N. K. Garg, Regioselective reactions of 3,4-pyridynes enabled by the aryne distortion model, *Nat. Chem.*, 2013, **5**, 54–60.

51 T. C. McMahon, J. M. Medina, Y.-F. Yang, B. J. Simmons, K. N. Houk and N. K. Garg, Generation and regioselective trapping of a 3,4-piperidine for the synthesis of functionalized heterocycles, *J. Am. Chem. Soc.*, 2015, **137**, 4082–4085.

52 M. Ramirez, D. Svatoněk, F. Liu, N. K. Garg and K. N. Houk, Origins of *endo* selectivity in Diels–Alder reactions of cyclic allene dienophiles, *Angew. Chem., Int. Ed.*, 2021, **60**, 14989–14997.

53 R. V. Viesser, C. P. Donald, J. A. May and J. I. Wu, Can twisted double bonds facilitate stepwise [2 + 2] cycloadditions?, *Org. Lett.*, 2024, **26**, 3778–3783.

54 E. Picazo, S. M. Anthony, M. Giroud, A. Simon, M. A. Miller, K. N. Houk and N. K. Garg, Arynes and cyclic alkynes as synthetic building blocks for stereodefined quaternary centers, *J. Am. Chem. Soc.*, 2018, **140**, 7605–7610.

55 S. Liu, Y. Li and Y. Lan, Mechanistic study of the fluoride-induced activation of a Kobayashi precursor: Pseudo-S<sub>N</sub>2 pathway via a pentacoordinated silicon ate complex, *Eur. J. Org. Chem.*, 2017, **2017**, 6349–6353.

56 S. Bhattacharjee, S. Deswal, N. Manoj, G. Jindal and A. T. Biju, Aryne three-component coupling involving CS<sub>2</sub> for the synthesis of S-aryl dithiocarbamates, *Org. Lett.*, 2021, **23**, 9083–9088.

57 A study of the mechanism for Kobayashi eliminations to form cyclic allenes will be reported elsewhere, as the systems are sufficiently complex to warrant independent investigation using experimental and computational techniques.

58 F. Scardiglia, J. D. Roberts, Evidence for cyclohexyne as an intermediate in the coupling of phenyllithium with 1-chlorocyclohexene, *Tetrahedron*, 1957, **1**, 343–344.

59 G. Wittig and P. Fritze, On the intermediate occurrence of 1,2-cyclohexadiene, *Angew. Chem., Int. Ed.*, 1966, **5**, 846.

60 R. Keese and E.-P. Krebs, Concerning the existence of 1-norbornene, *Angew. Chem., Int. Ed. Engl.*, 1971, **10**, 262–263.

61 For computational ease and to allow for comparisons, calculations were performed using trimethylsilyltriflate substrates. In practice, different silicon substituents and different sulfonates are commonly used in Kobayashi eliminations.

62 O. Smith, M. J. Hindson, A. Sreenithya, V. Tataru, R. S. Paton, J. W. Burton and M. D. Smith, Harnessing triaryloxonium ions for aryne generation, *Nat. Synth.*, 2024, **3**, 58–66.

63 As strained intermediate generation from Kobayashi precursors has been achieved using a variety of fluoride counterions (e.g., Cs<sup>+</sup>, K<sup>+</sup>, and NBu<sub>4</sub><sup>+</sup>), the role of the counterion was omitted from our



studies. Additionally, the role of cations is further complicated by the possibility of cation exchange in many reactions, as well as possible solvent-cation interactions.

64 Prior computational studies done at the B3LYP/6-31G(d)/SMD(MeCN) level of theory by Li and Lan report that the elimination to give **3** is favourable by  $-31.4 \text{ kcal mol}^{-1}$  (see ref 55). A more recent study by Jindal and Biju performed using M06-2X-D3/def2-TZVPP/SMD(THF)//M06-2X-D3/6-31G(d,p) gave the corresponding  $\Delta G$  of  $-16.2 \text{ kcal mol}^{-1}$  (see ref 56).

65 K. Balaraman and C. Wolf, Chemodivergent Csp<sup>3</sup>-F bond functionalization and cross-electrophile alkyl-alkyl coupling with alkyl fluorides, *Science Advances*, 2022, **8**, eabn7819.

66 We have verified the formation of SiMe<sub>3</sub>F by <sup>1</sup>H and <sup>19</sup>F NMR spectroscopy; see the ESI for details.

67 E. Yoshioka, K. Kakigi, S. Miyoshi, Y. Kawasaki and H. Miyabe, Aryne precursors for selective generation of 3-haloarynes: Preparation and application to synthetic reactions, *J. Org. Chem.*, 2020, **85**, 13544–13556.

68 C. Hall, J. L. Henderson, G. Ernouf and M. F. Greaney, Tandem thia-Fries rearrangement – Cyclisation of 2-(trimethylsilyl)phenyl trifluoromethanesulfonate benzyne precursors, *Chem. Commun.*, 2013, **49**, 7602–7604.

69 O. K. Rasheed, I. R. Hardcastle, J. Raftery and P. Quayle, Aryne generation vs. Truce-Smiles and Fries rearrangements during the Kobayashi fragmentation reaction: A new bi-aryl synthesis, *Org. Biomol. Chem.*, 2015, **13**, 8048–8052.

70 J. M. Medina, M. K. Jackl, R. B. Susick and N. K. Garg, Synthetic studies pertaining to the 2,3-pyridyne and 4,5-pyrimidine, *Tetrahedron*, 2016, **72**, 3629–3634.

71 J. P. H. Charmant, A. M. Dyke and G. C. Lloyd-Jones, The anionic thia-Fries rearrangement of aryl triflates, *Chem. Commun.*, 2003, 380–381.

72 In cases where the thia-Fries rearrangement is observed, we suspect there are subtle structural factors that stabilize the aryl anion and/or destabilize the elimination pathway.

73 When reacted under highly protic conditions (*t*-BuOH (50 equiv), CsF (5.0 equiv), MeCN, 40°C), 2,3-naphthalene precursor (2-(trimethylsilyl)-3-naphthyl trifluoromethanesulfonate) undergoes protodesilylation, along with presumed aryne generation and other undesired pathways, resulting in the formation of 2-naphthyl trifluoromethanesulfonate (see ESI, section E).

74 We also considered direct E2-like elimination of the silicate intermediate in both cases but were unable to locate transition states for those possible pathways. However, in our computational studies of a substituted cyclic 1,2,3-triene and its Kobayashi precursor (see ESI, section H for details), the barrier for this type of direct elimination was located. The barrier for the silicate intermediate undergoing direct elimination was found to be higher than the barrier for vinyl anion formation, supporting the notion that vinyl anion formation is the preferred pathway.

75 Prior studies have shown this carbanion is not a stationary point on the potential energy surface and undergoes spontaneous elimination upon attempted geometry optimization; see: G. W. Breton and J. V. Riddlehoover, Spontaneous formation of strained anti-Bredt bridgehead alkenes upon computational geometry optimization of bicyclic  $\beta$ -halo carbanions, *Organics*, 2024, **5**, 205–218.

76 The aliphatic anion is expected to be  $10^5$ – $10^{10}$  times less stable than those seen in the previously discussed systems, as aryl and vinyl

anions have  $pK_a$  values roughly 5–10 units lower than aliphatic anions.

77 Calculations were performed in MeCN as this is a common solvent for strained intermediate generation.

78 Optimization of the starting silyltriflate **32** and silicate **33** were performed using dihedral constraints on the Si–C–C–O bond set to the given angle. See ESI, section L for further details.

79 C. H. DePuy, R. D. Thurn and G. F. Morris, Concerted bimolecular eliminations and some comments on the effect of dihedral angle on E2 reactions, *J. Am. Chem. Soc.*, 1962, **84**, 1314–1315.

80 In unconstrained aliphatic systems, free rotation or conformational changes may be readily achieved, which may render such calculations unnecessary. Thus, what we propose is likely most valuable on rigid or otherwise constrained systems, such as anti-Bredt olefins.

81 This present study is limited to the aliphatic systems shown that do not possess adjacent substituents that could plausibly stabilize an intermediate alkyl anion, such as ketones, olefins, or aromatic rings. In such cases, the mechanisms may vary depending on the exact substrate.



Full details on the computational methods are accessible in the ESI.

